Electronic Supplementary Material (ESI) for Materials Chemistry Frontiers.

Supporting Information

"Turn-on" Fluorescence Sensor for Organic Amines Fabricated via Sustainable Processing

Renjian Hu [a], Shiyun Lin [b], Danning Hu [a], Hongye Huang [a], Mengshi Wang [a], Ruoxin Li [a], Mei Tian [c], Zhigang Shuai [b] and Yen Wei *[ad]

[a] *The Key Laboratory of Bioorganic Phosphorus Chemistry & Chemical Biology, Department of Chemistry, Tsinghua University, Beijing 100084, China.*
[b] *MOE Key Laboratory of Organic Optoelectronics and Molecular Engineering, Department of Chemistry, Tsinghua University, Beijing 100084, China.*
[c] *Department of Nuclear Medicine and PET Center, The Second Affiliated Hospital of Zhejiang University School of Medicine, Hangzhou 310009, China.*
[d] *Department of Chemistry, Center for Nanotechnology and Institute of Biomedical Technology, Chung-Yuan Christian University, Chung-Li 32023, Taiwan, China.*

E-mail: weiyen@mail.tsinghua.edu.cn (Y. Wei)

TABLE OF CONTENTS

1. **General information**
2. **Synthesis of pre-DiCat**
3. **Synthesis of DiCat**
4. **NMR spectra**
5. **MALDI-TOF-MS**
6. **FT-IR spectra**
7. **UV-Vis spectra**
8. **Optimization of the detection condition**
9. **Control experiments**
10. **Fluorescence spectrum of unknown samples containing Et_3N**
11. **Fluorescence spectrum and fitting curves of diverse organic amines**
12. **Selectivity of this detection protocol**
13. **Computational details**

General information

All the reagents were purchased and used directly without further purification. Thin layer chromatography (TLC) was performed on EMD preloaded plated (silica gel 60 F254) and visualized with hand-hold UV lamp at 254 or 365 nm.

^{1}H-NMR (400 MHz) and ^{13}C-NMR (101 MHz) spectra were measured on Bruker spectrometer. Chemical shifts were expressed in parts per million (ppm) with respect to internal standard of TMS. Coupling constants were reported as Hertz (Hz), signal shapes and splitting patterns were indicated as follows: s, singlet; d, doublet; t, triplet; q, quartet; m, multiplet. Mass spectra data were collected on MALDI-TOF MS Performance (Shimadzu, Japan).

IR spectra were recorded with Perkin Elmer (Spectrum 100) FT-IR Spectrometer with attenuated total reflectance (ATR) accessory. UV-visible spectra were collected on Perkin Elmer (Lambda 750) UV/Vis/NIR Spectrometer using THF or THF/H_2O solution in quartz cuvette. Fluorescence spectra were recorded by SHIMADZU Spectro fluorophotometer RF-6000 using THF or THF/H_2O solution in quartz cuvette at specific excitation wavelength.

Synthesis of pre-DiCat

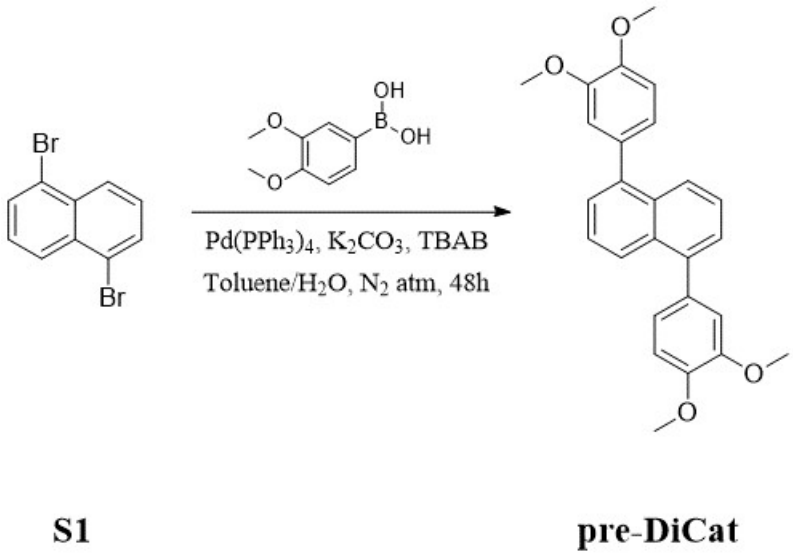

Figure S1 Synthetic procedure for **pre-DiCat**

Round-bottom flask equipped with a magnetic stirrer was charged with 1,5-dibromonaphthalene (2.86g, 10 mmol), (3,4-dimethoxyphenyl)boronic acid (4.00 g, 22 mmol), anhydrous K_2CO_3 (6.91 g, 50 mmol), TBAB (665 mg, 2.0 mmol), Pd(PPh3)4 (116 mg, 0.10 mmol). The flask was evacuated and filled with N_2 for three times before the addition of 80 mL toluene and 25 mL DI H_2O. The reaction mixture was vigorously stirred at 90 cent. for 48h and then cooled to room temperature before post-treatment. Adding DI H_2O into reaction mixture gradually and extracting with EA for three times. The combined organic layer was washed with brine and dried with anhydrous Na_2SO_4 before being concentrated under reduced pressure to afford the crude product. It was further purified by washing with EA, PE and DCM for several times to give 1,5-bis(3,4-dimethoxyphenyl)naphthalene (**pre-DiCat**) (3.60 g, 90.0%) as white powder. **^{1}H-NMR** (400 MHz, DMSO-*d6*) δ = 7.91 (d, J = 8.3 Hz, 2H), 7.56 (t, J = 7.6 Hz, 2H), 7.48 (d, J = 6.9 Hz, 2H), 7.16 (d, J = 8.2 Hz, 2H), 7.09 (s, 2H), 7.05 (d, J = 8.9 Hz, 2H), 3.89 (s, 6H), 3.84 (s, 6H). **^{13}C-NMR** (101 MHz, DMSO-*d6*) δ = 149.22, 148.91, 140.56, 133.44, 132.22, 127.34, 126.19, 125.59, 122.61, 114.30, 112.48, 56.26, 56.22. **MALDI-TOF-MS** m/z calculated for $C_{26}H_{24}O_4$ [M]+ 400.2, found 400.2. **m.p.** 184-190 cent.

Synthesis of DiCat

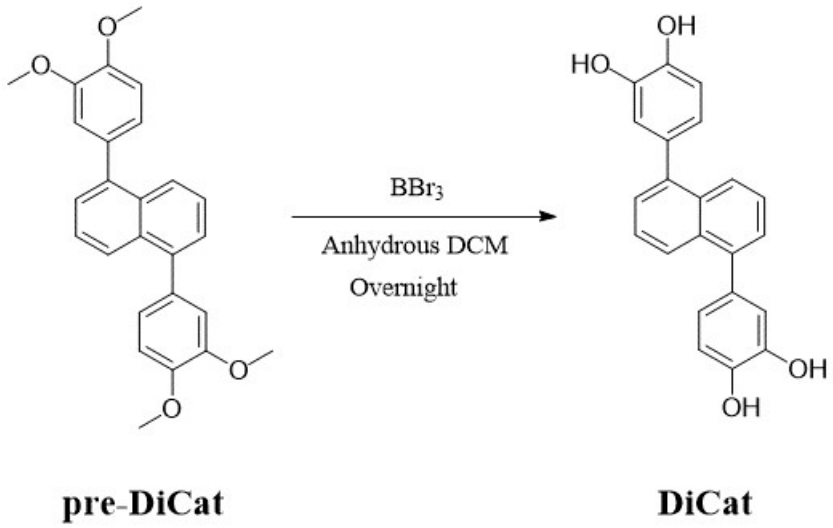

Figure S2 Synthetic procedure for **DiCat**

A flame-dried round-bottom flask equipped with a magnetic stirrer was charged with **pre-DiCat** (4.00 g, 10 mmol). It was evacuated and filled with N_2 for three times before the addition of 100 mL extra dry DCM. BBr_3 (10.0 g, 40 mmol) was dissolved in extra dry DCM and added into the reaction mixture dropwise at -78 cent.. The solution was allowed to warm to R.T. and stirred overnight. DI H_2O was gradually added to quench excess amount of BBr_3. Reaction mixture was filtrated with Buchner funnel and washed with DI H_2O several times to afford crude product. Transferring the filter residue into another flask and adding EA to disperse the impure sample. It was ultrasonicated for 5 minutes before centrifugation. This process was repeated for several times and white solid (2.84 g, 82.7%) was obtained after drying under vacuum oven for 24h. **^{1}H-NMR** (400 MHz, acetone-*d6*) δ = 8.08 (s, 2H), 8.03 (s, 2H), 7.91 (d, J = 8.5 Hz, 2H), 7.49 – 7.40 (m, 2H), 7.36 (d, J = 6.7 Hz, 2H), 6.98 – 6.94 (m, 4H), 6.81 (dd, J = 8.0, 1.9 Hz, 2H). **^{13}C-NMR** (101 MHz, acetone-*d6*) δ = 144.97, 144.74, 140.70, 132.87, 132.37, 126.58, 125.26, 121.62, 117.17, 115.27. **MALDI-TOF-MS** m/z calculated for $C_{22}H_{16}O_4$ [M]+ 344.1, found 344.2. **m.p.** ＞300 cent.

NMR spectra

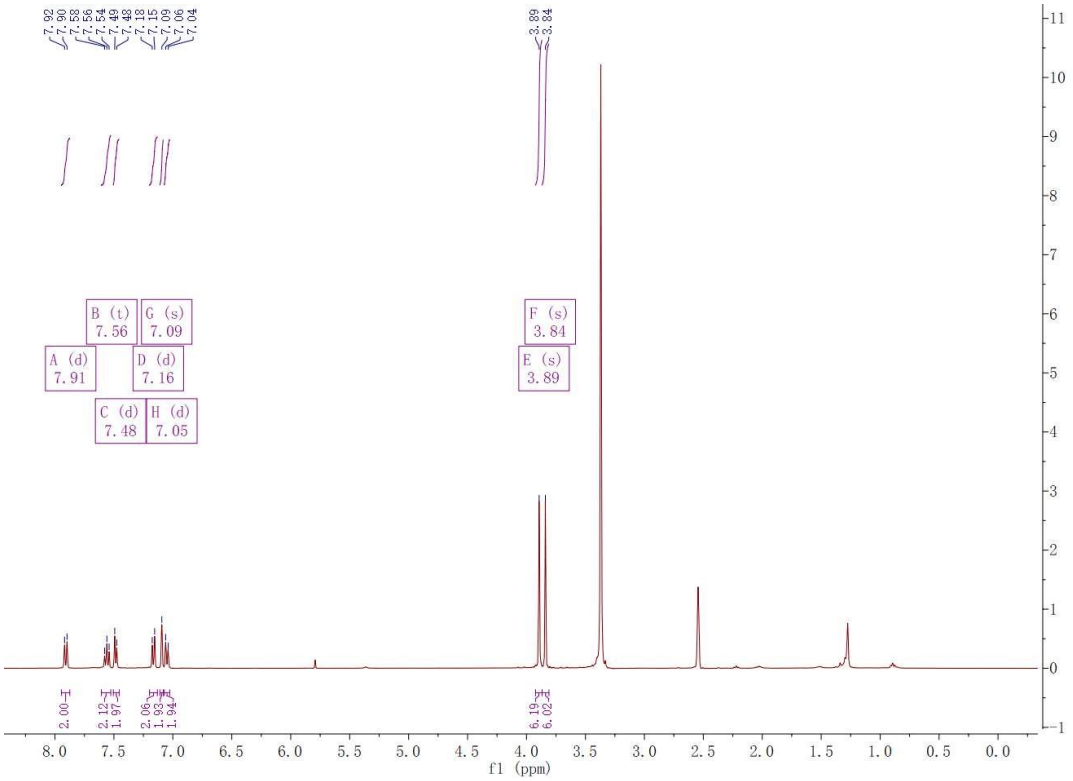

Figure S3 ^{1}H-NMR spectrum of **pre-DiCat**

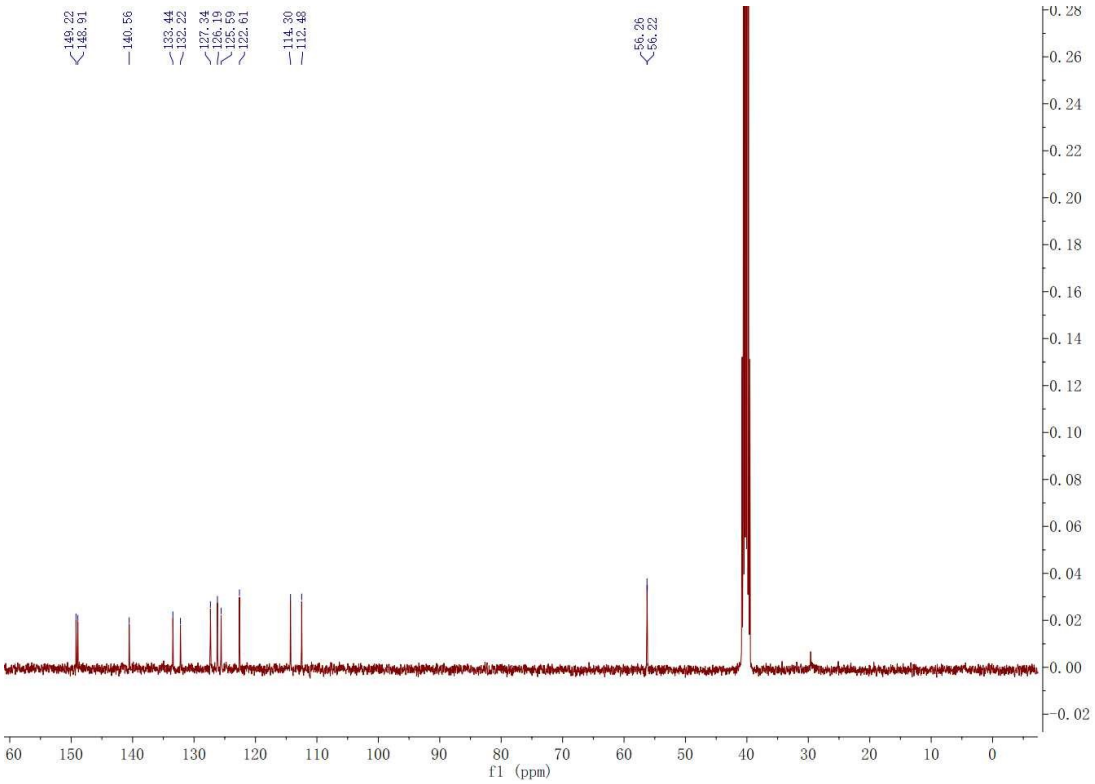

Figure S4 ^{13}C-NMR spectrum of **pre-DiCat**

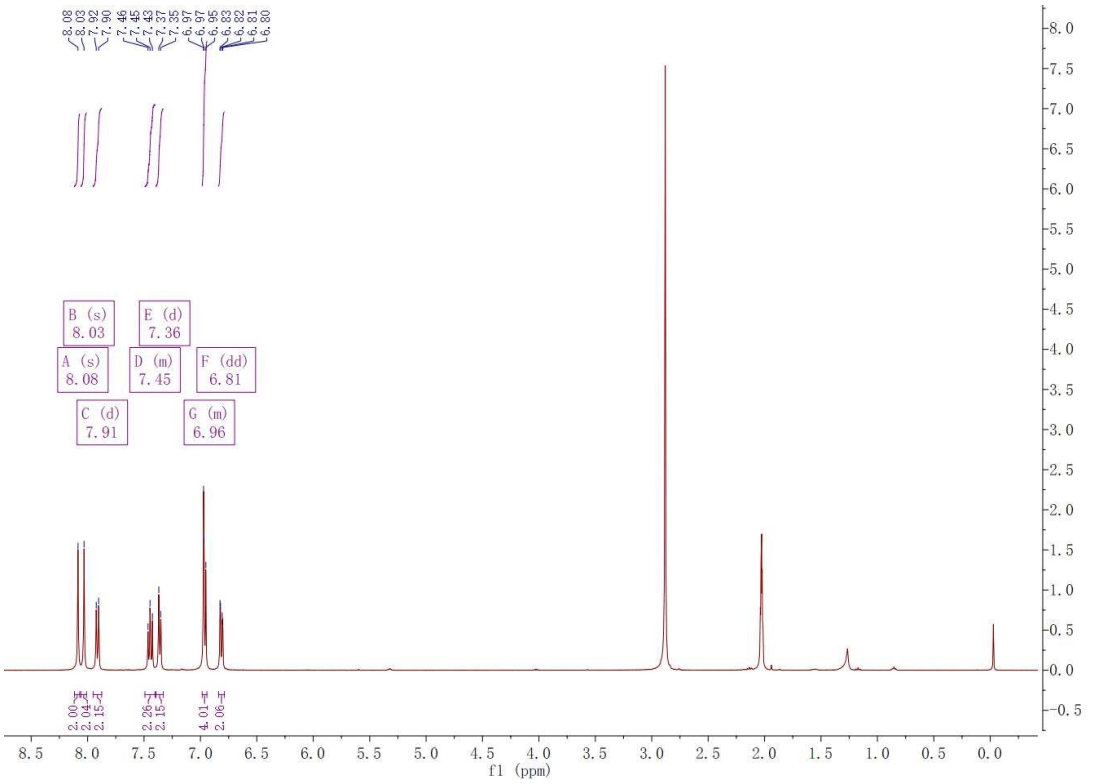

Figure S5 ^{1}H-NMR spectrum of **DiCat**

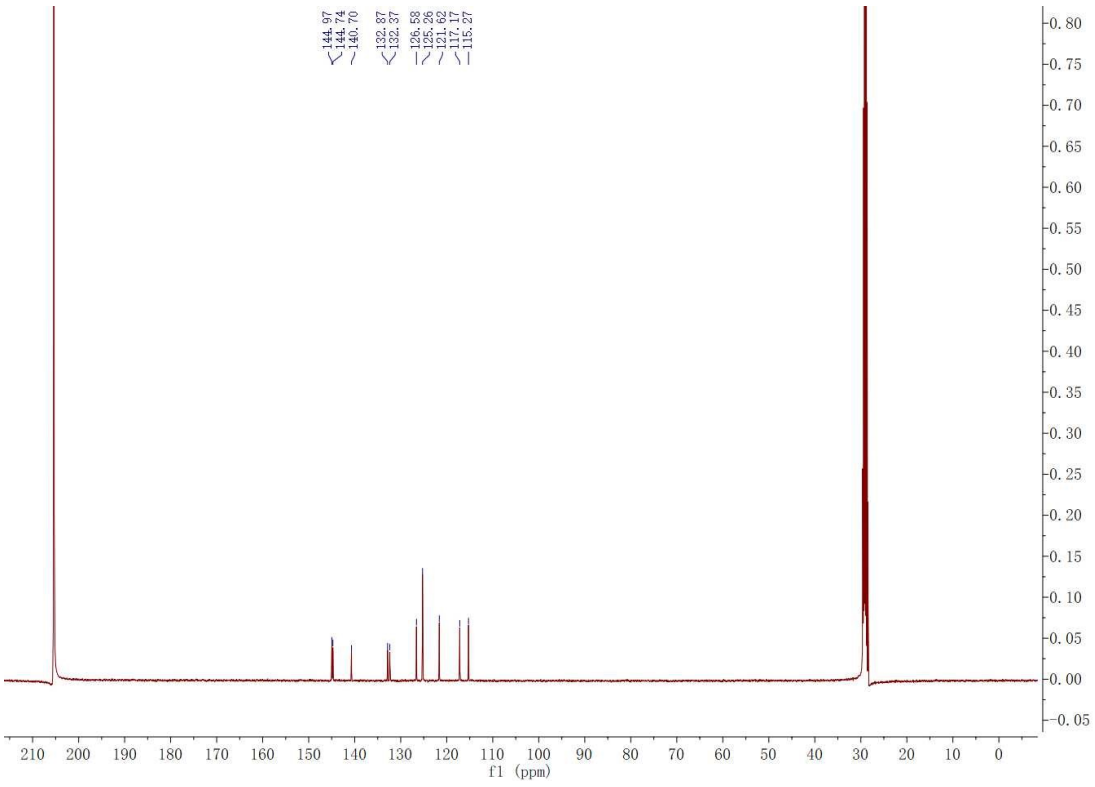

Figure S6 ^{13}C-NMR spectrum of **DiCat**

MALDI-TOF-MS

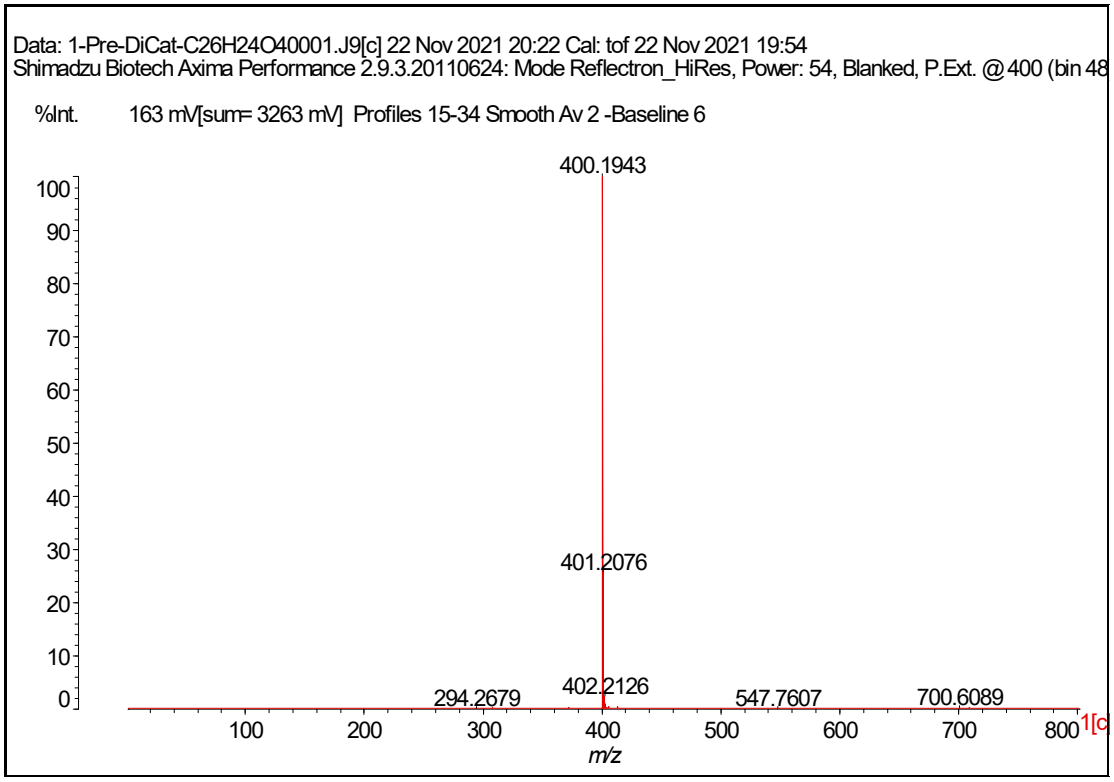

Figure S7 MALDI-TOF-MS record of **pre-DiCat**

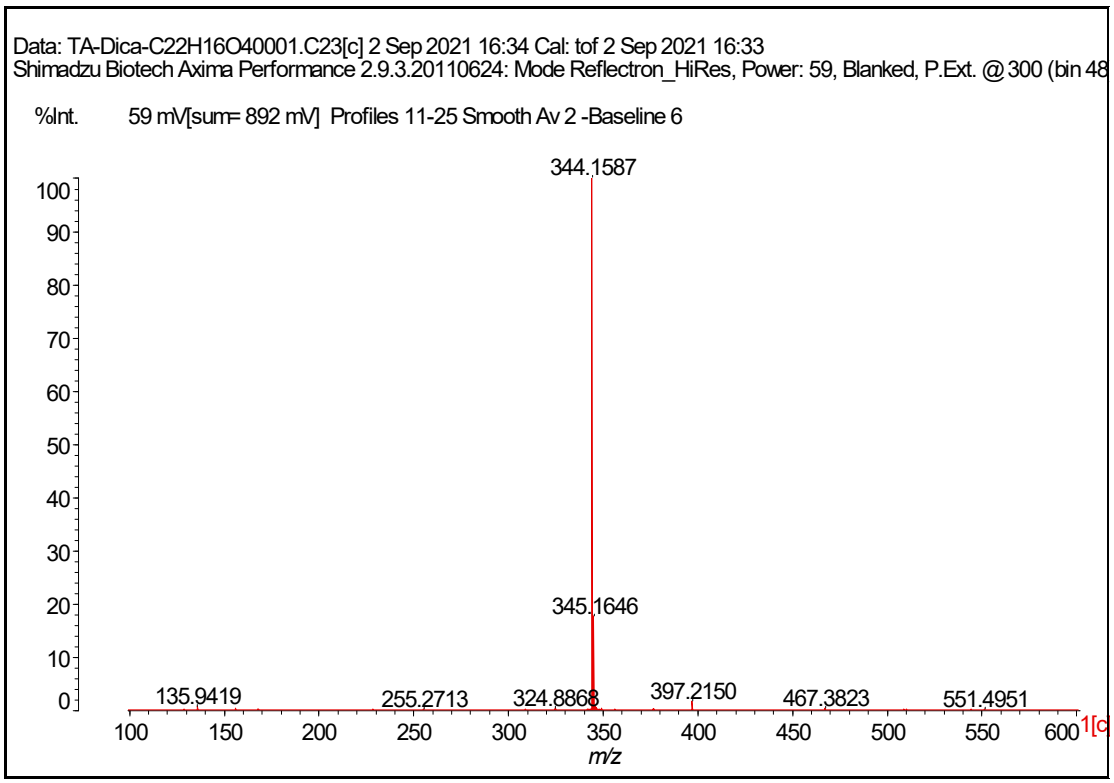

Figure S8 MALDI-TOF-MS record of **DiCat**

FT-IR spectra

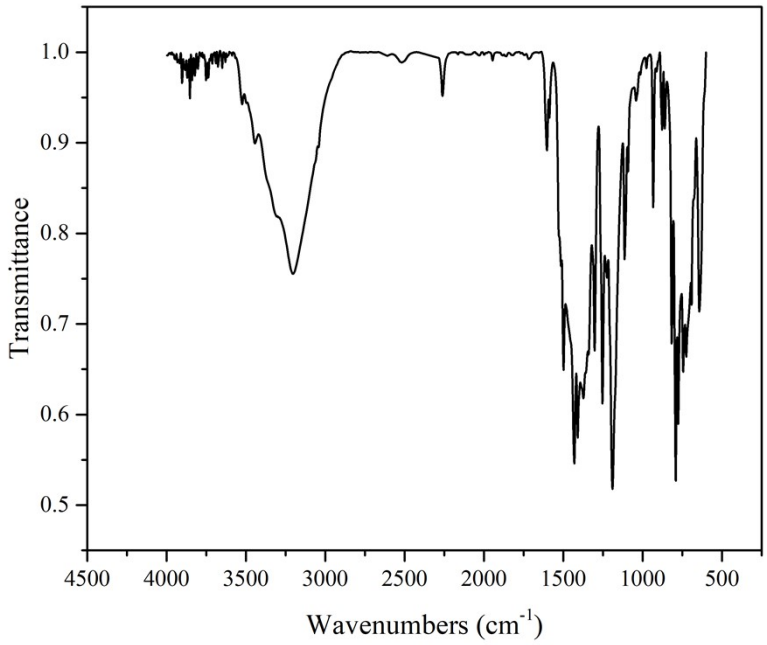

Figure S9 FT-IR spectrum of **pre-DiCat**

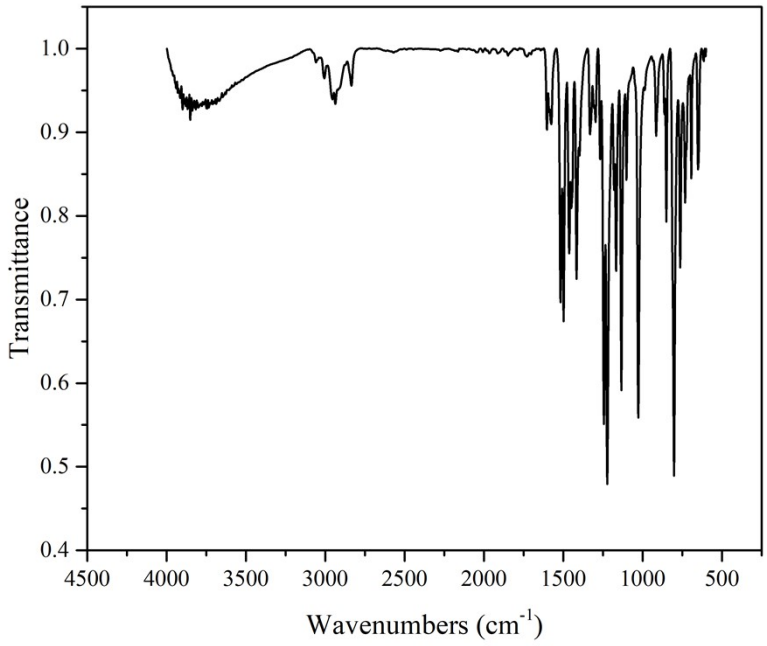

Figure S10 FT-IR spectrum of **DiCat**

UV-Vis spectra

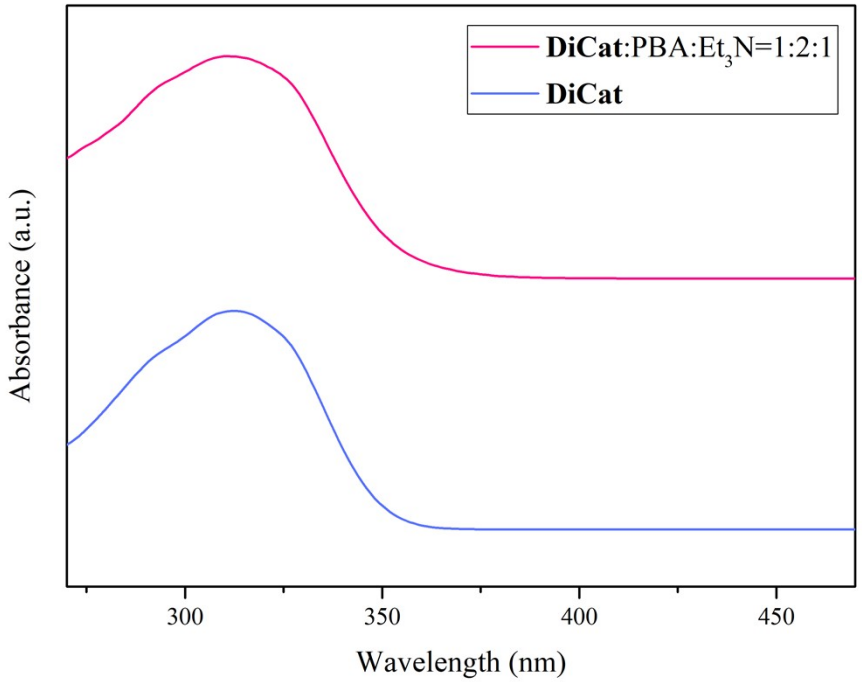

Figure S11 UV-Vis spectrum of **DiCat** and sensing system under optimal detection condition (binary solvent of THF and DI H_2O, water fraction of 70%).

Optimization of the detection condition

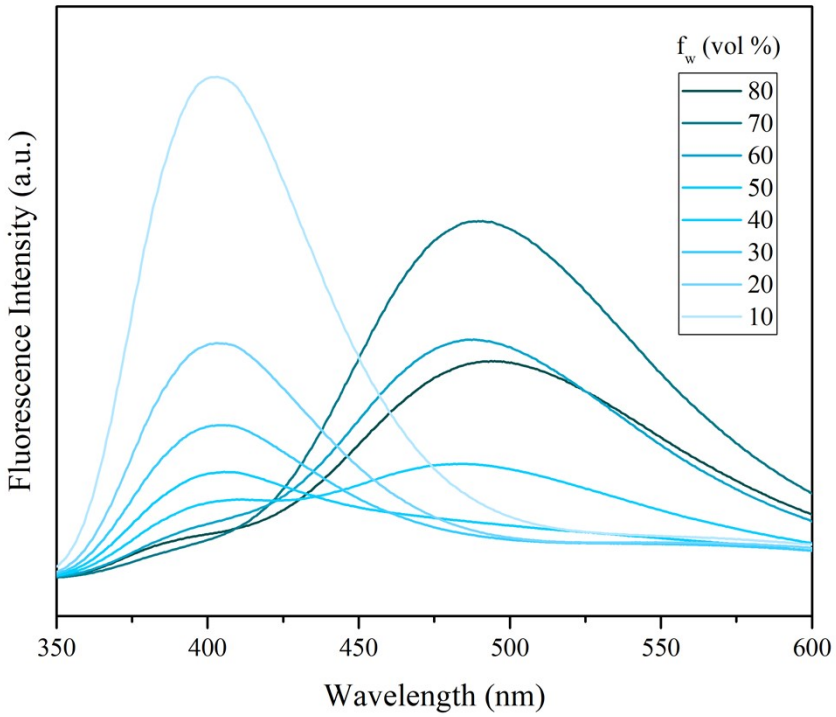

Figure S12 Fluorescence spectrum recorded in THF/DI H_2O solution of DiCat/PBA/Et3N (molar ratio 1:2:1) with varying water fraction.

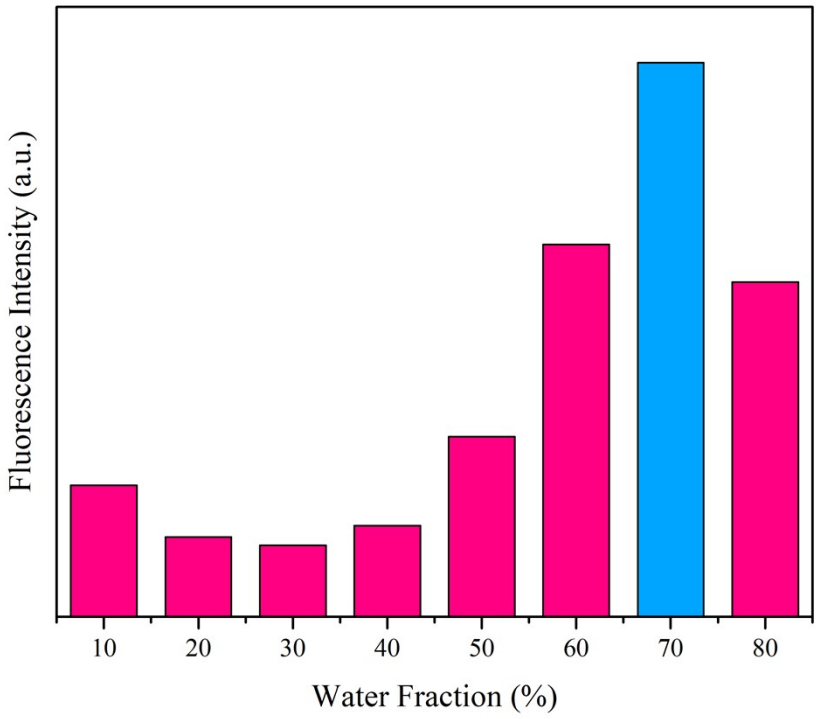

Figure S13 Column chart of PL intensity versus water fraction which determines 70% water fraction as the optimal detection condition.

Control experiments

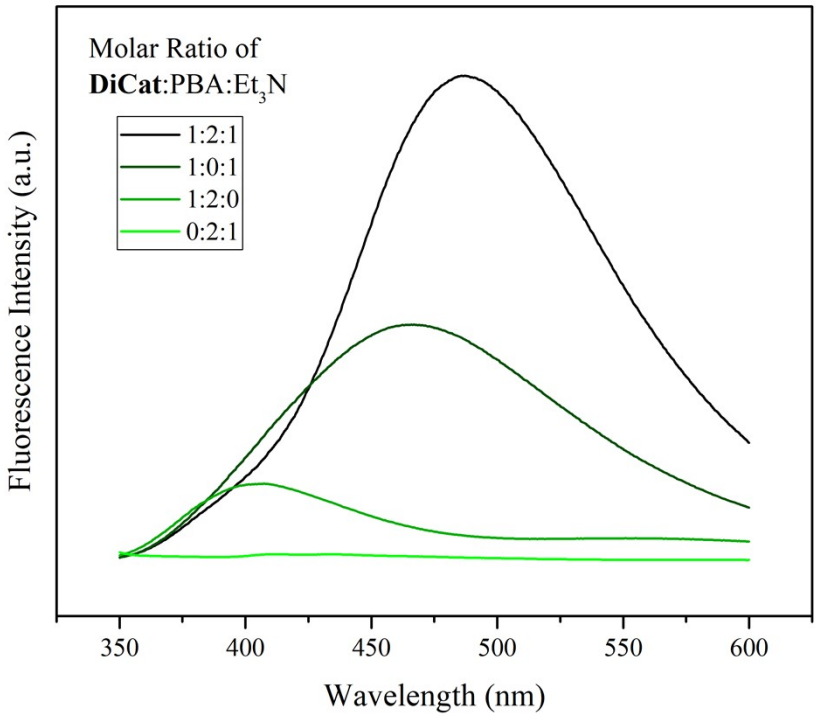

Figure S14 Fluorescence spectrum of **DiCat**/PBA/Et_3N system with different molar ratio in THF/DI H_2O binary solvent (f_w = 70%).

Fluorescence spectrum of unknown samples containing Et_3N

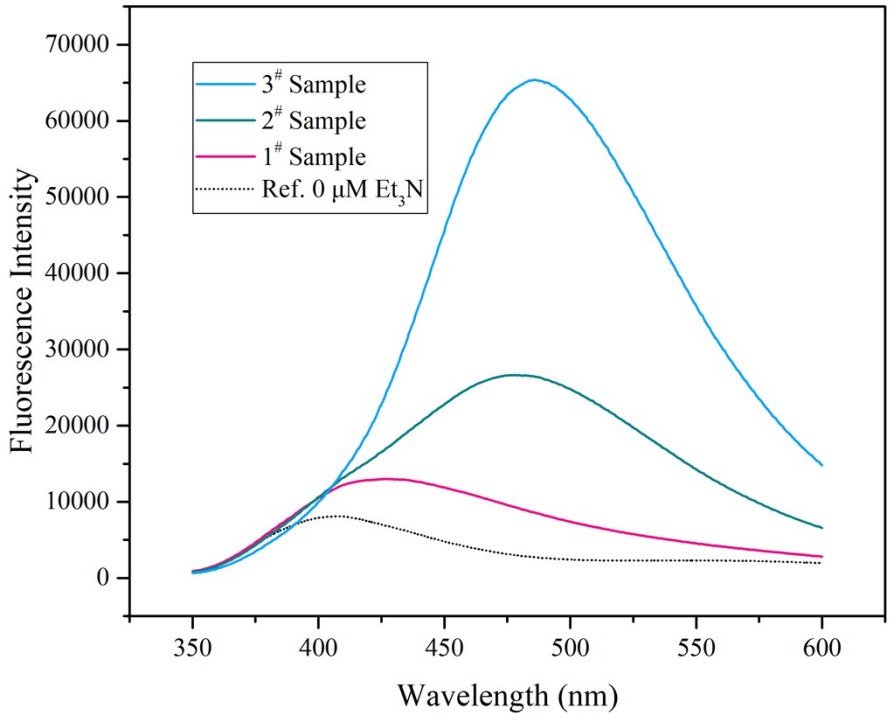

Figure S15 Fluorescence spectrum of three unknown samples containing Et_3N comparing with reference sensing system without Et_3N (recorded under optimal detection condition with THF/DI H2O binary solvent, f_w = 70%; concentration of **DiCat** is 100 μM; concentration of PBA is 200 μM).

Fluorescence spectrum and fitting curves of diverse organic amines

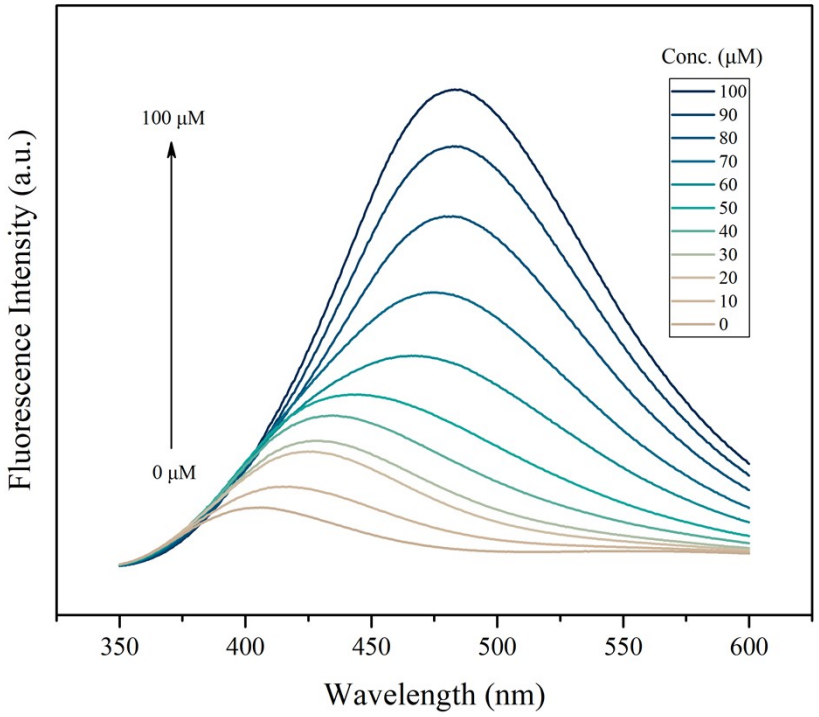

Figure S16 Fluorescence spectrum of **DiCat**/PBA with increasing concentration of diisopropylamine under optimal detection condition. (concentration of **DiCat** and PBA is fixed to be 100 μM and 200 μM respectively)

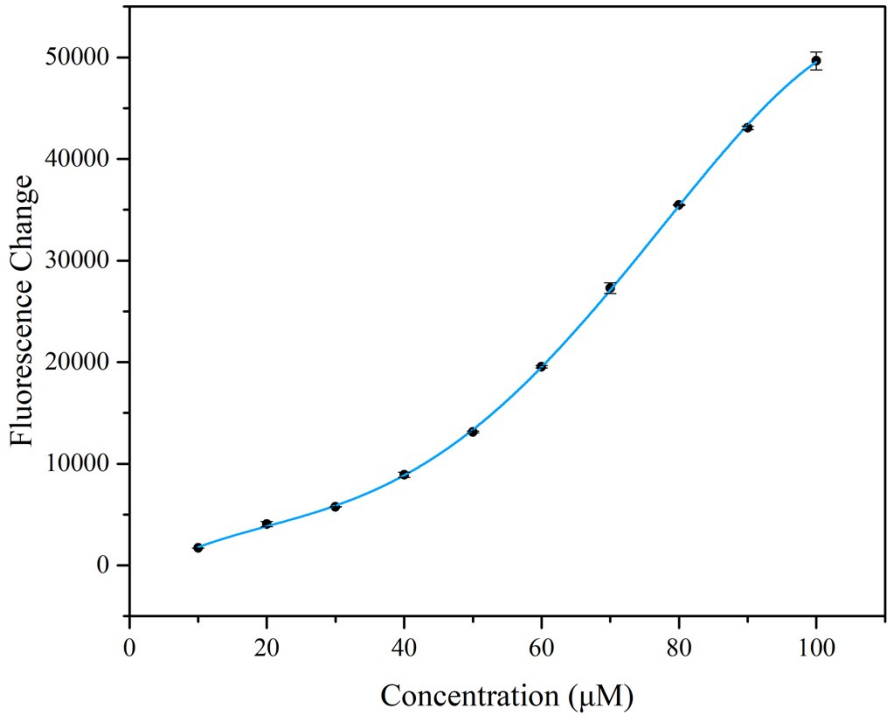

Figure S17 Polynomial regression of fluorescence change versus diisopropylamine concentration.

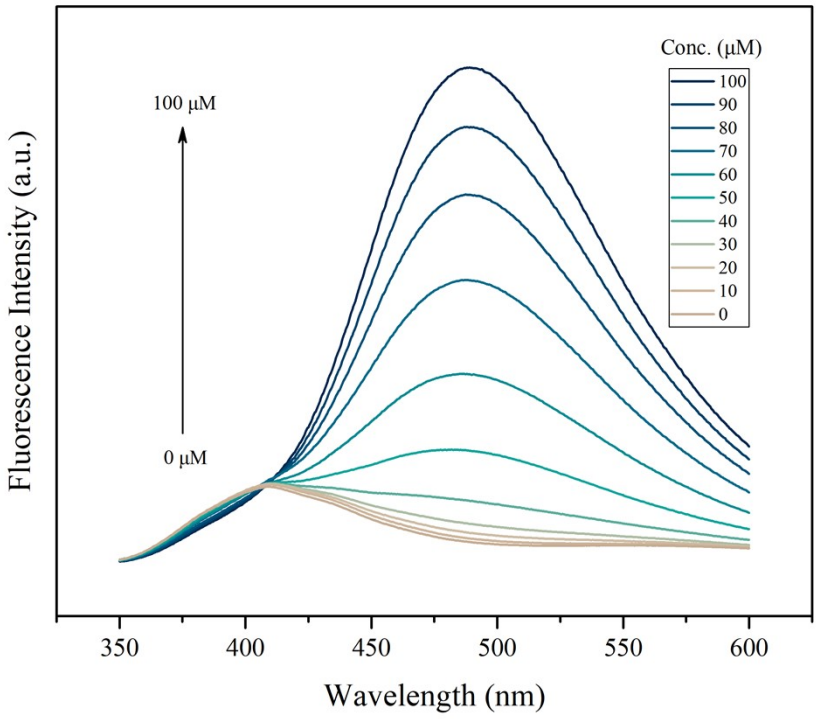

Figure S18 Fluorescence spectrum of **DiCat**/PBA with increasing concentration of n-butylamine under optimal detection condition. (concentration of **DiCat** and PBA is fixed to be 100 μM and 200 μM respectively)

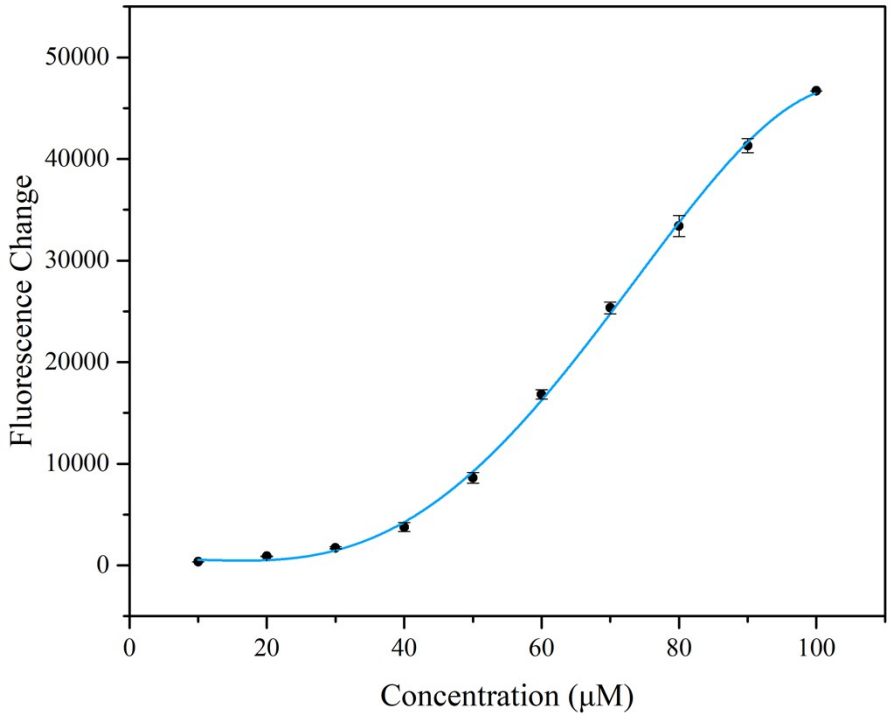

Figure S19 Polynomial regression of fluorescence change versus n-butylamine concentration.

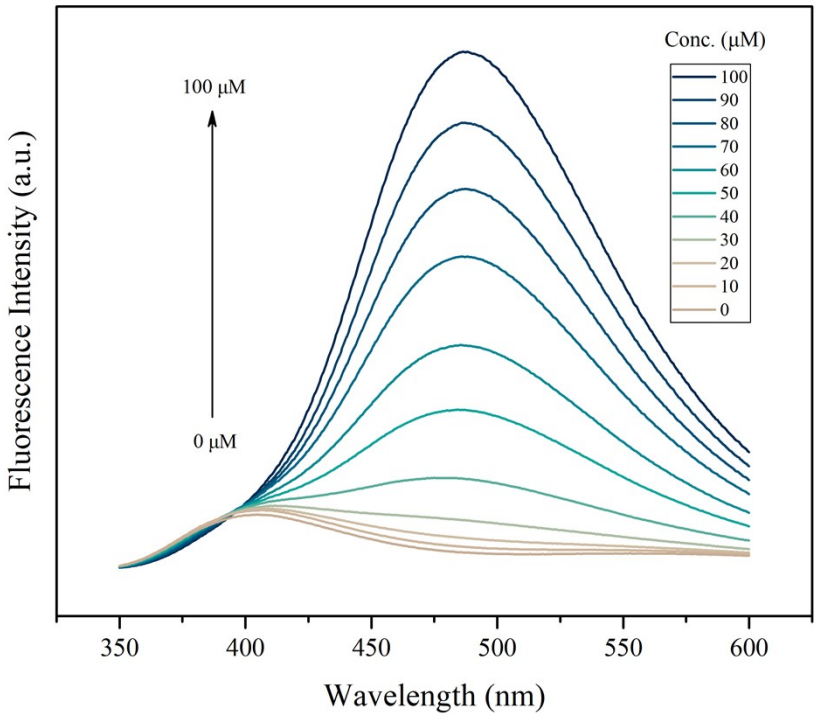

Figure S20 Fluorescence spectrum of **DiCat**/PBA with increasing concentration of DIPEA under optimal detection condition. (concentration of **DiCat** and PBA is fixed to be 100 μM and 200 μM respectively)

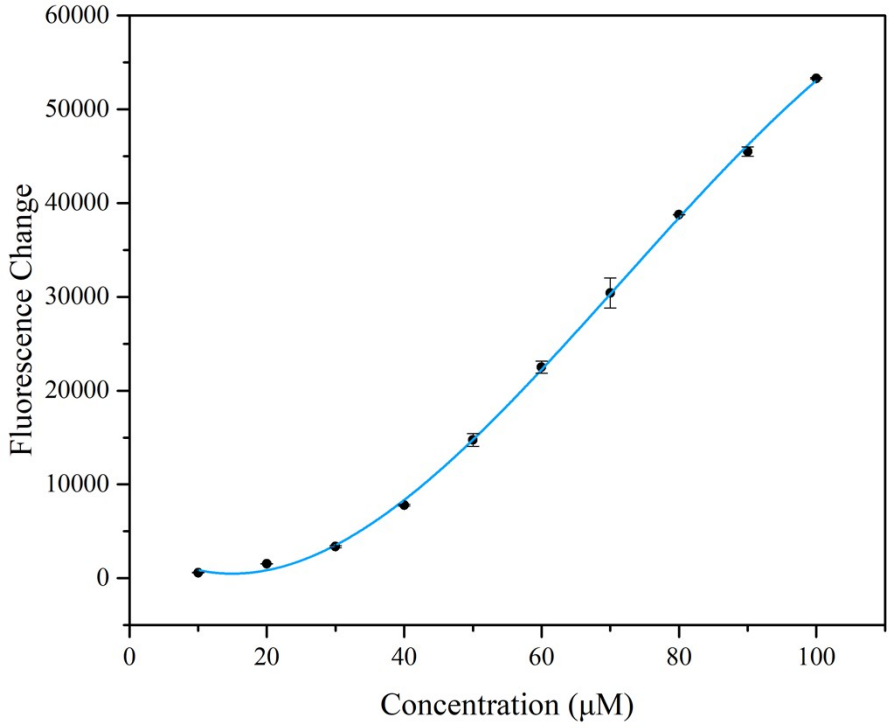

Figure S21 Polynomial regression of fluorescence change versus DIPEA concentration.

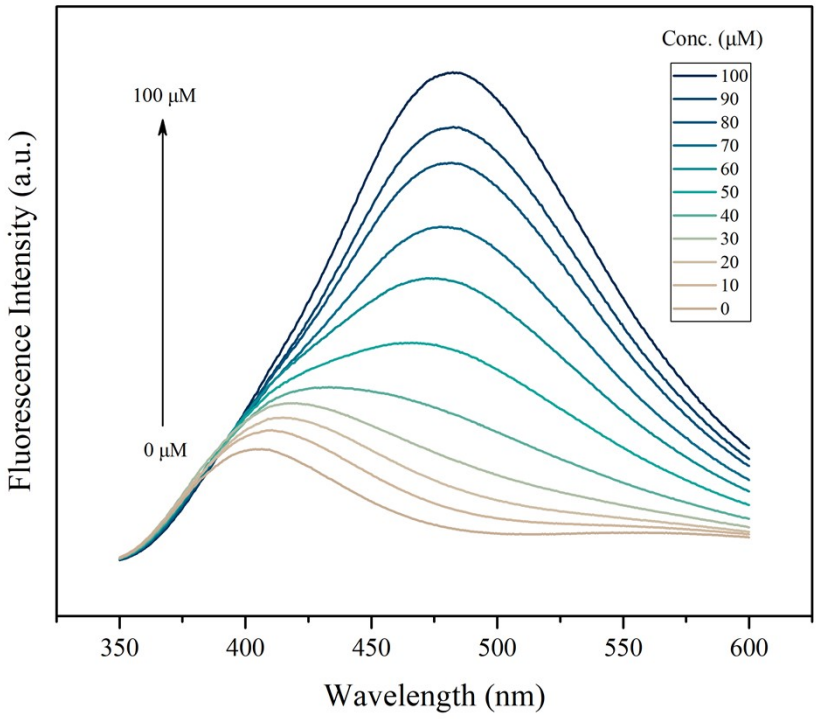

Figure S22 Fluorescence spectrum of **DiCat**/PBA with increasing concentration of DMAP under optimal detection condition. (concentration of **DiCat** and PBA is fixed to be 100 μM and 200 μM respectively)

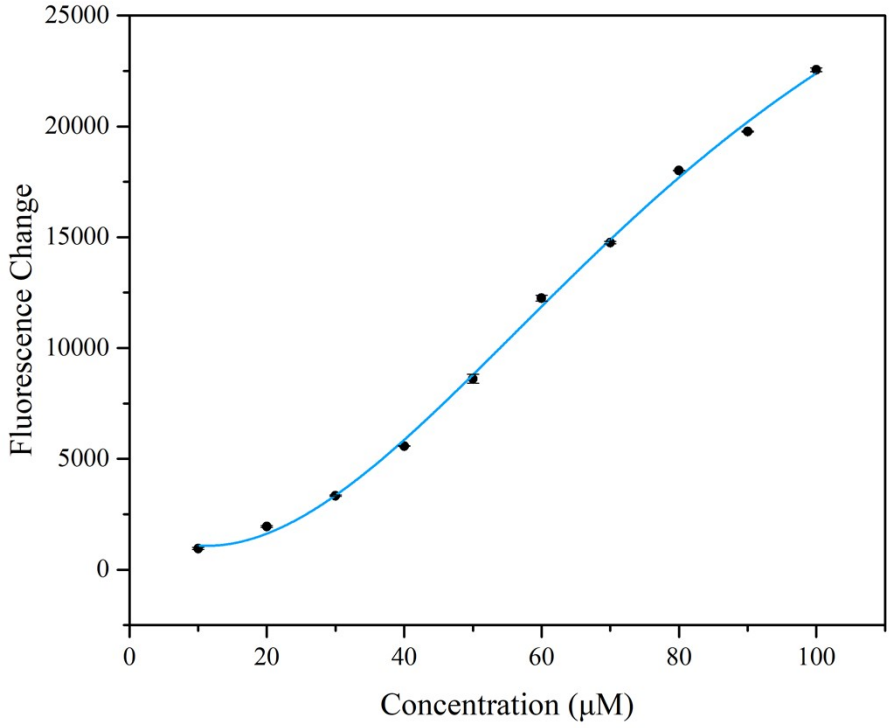

Figure S23 Polynomial regression of fluorescence change versus DMAP concentration.

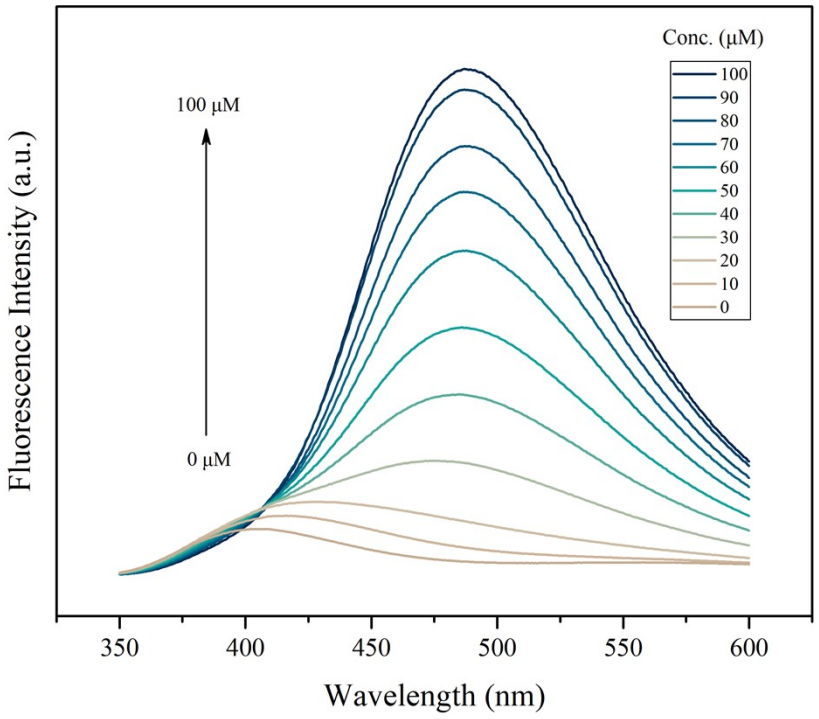

Figure S24 Fluorescence spectrum of **DiCat**/PBA with increasing concentration of putrescine under optimal detection condition. (concentration of **DiCat** and PBA is fixed to be 100 μM and 200 μM respectively)

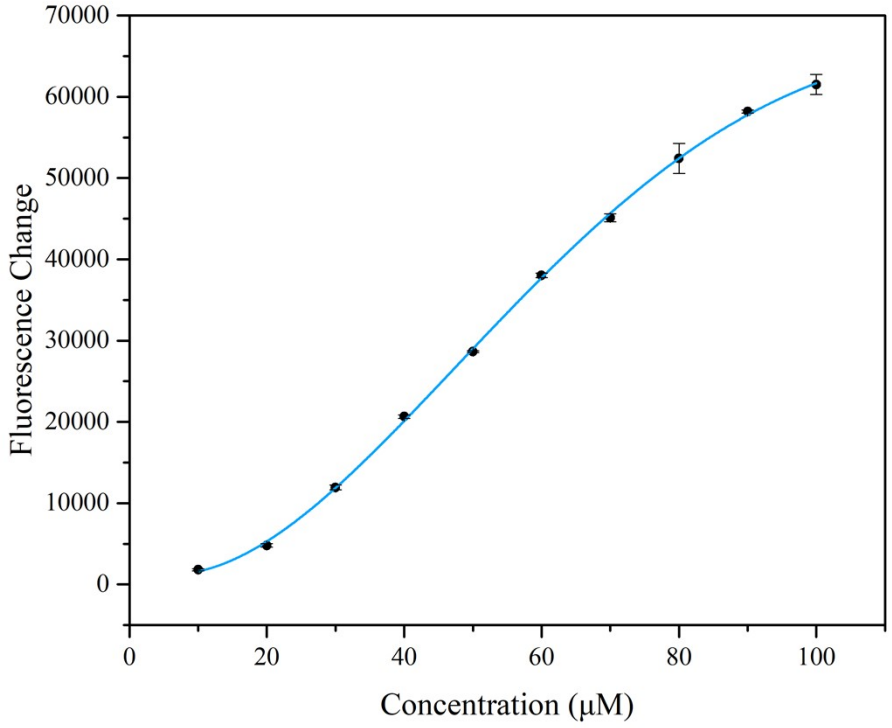

Figure S25 Polynomial regression of fluorescence change versus putrescine concentration.

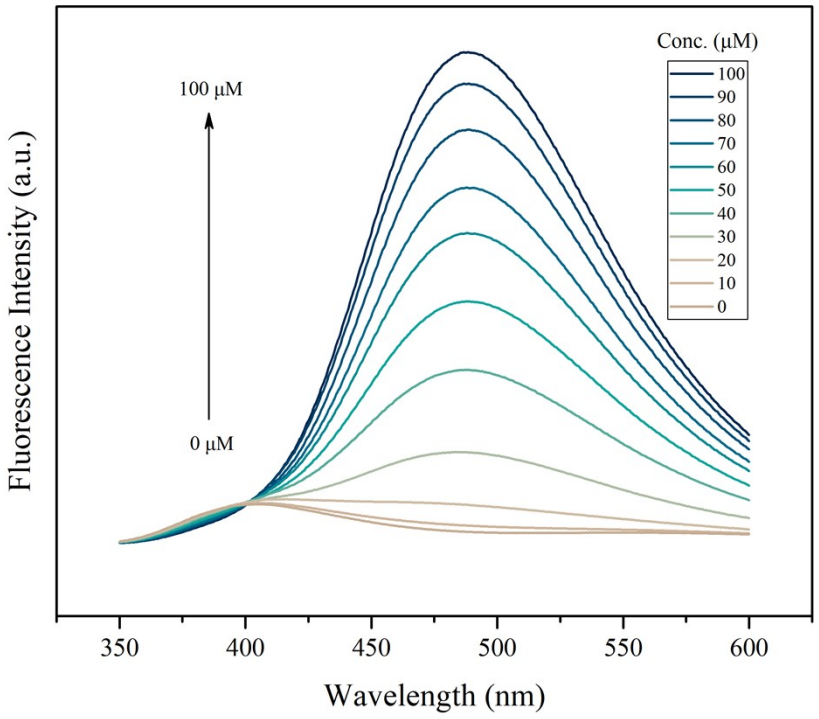

Figure S26 Fluorescence spectrum of **DiCat**/PBA with increasing concentration of cadaverine under optimal detection condition. (concentration of **DiCat** and PBA is fixed to be 100 μM and 200 μM respectively)

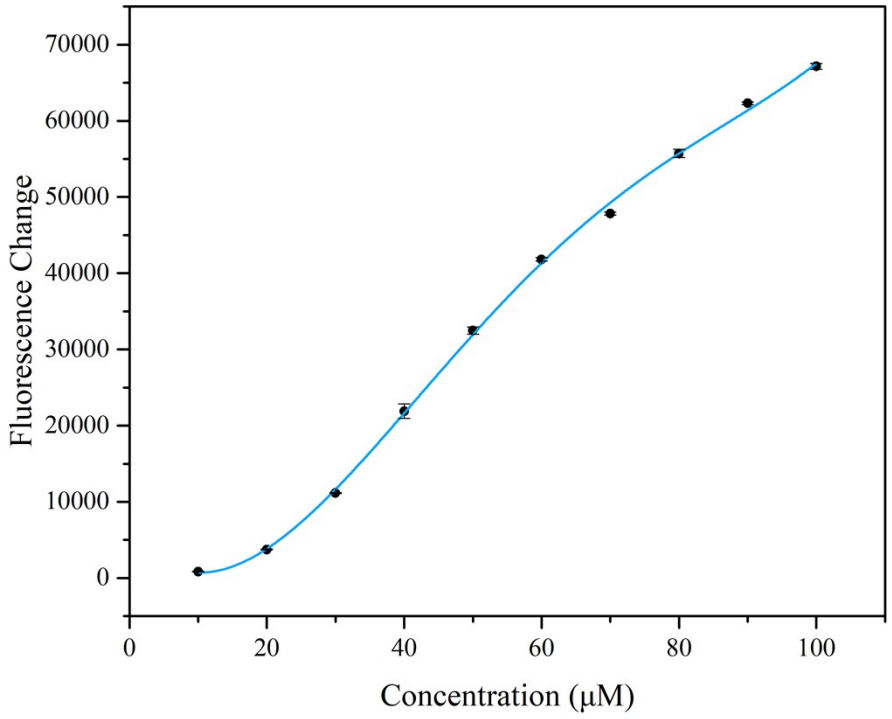

Figure S27 Polynomial regression of fluorescence change versus cadaverine concentration.

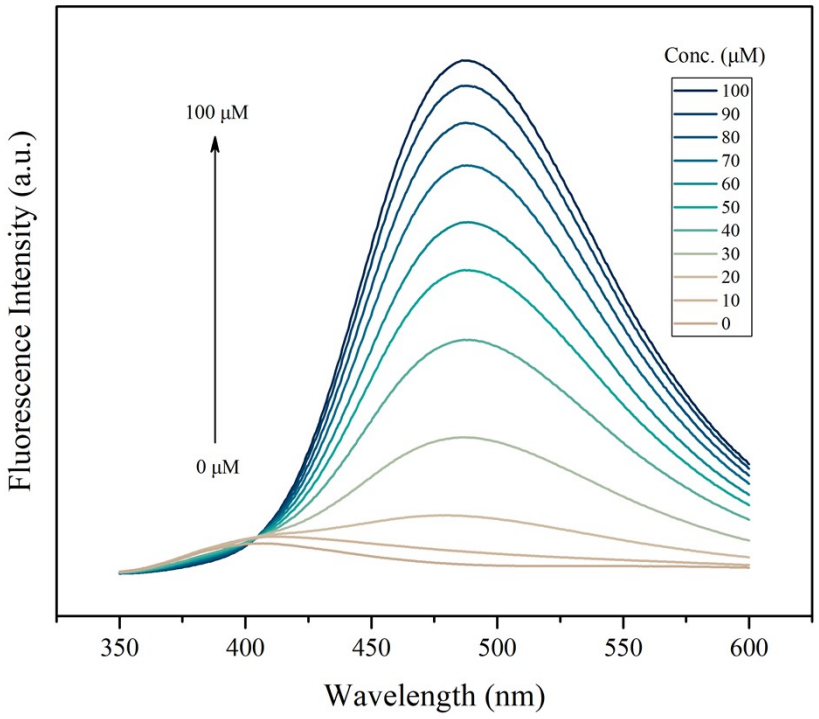

Figure S28 Fluorescence spectrum of **DiCat**/PBA with increasing concentration of spermine under optimal detection condition. (concentration of **DiCat** and PBA is fixed to be 100 μM and 200 μM respectively)

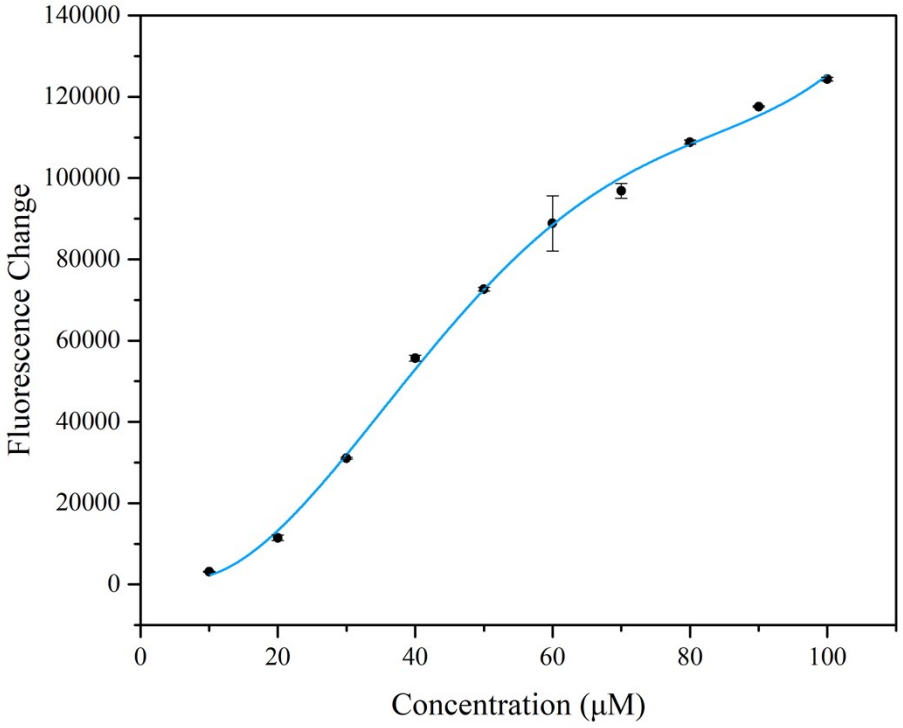

Figure S29 Polynomial regression of fluorescence change versus spermine concentration.

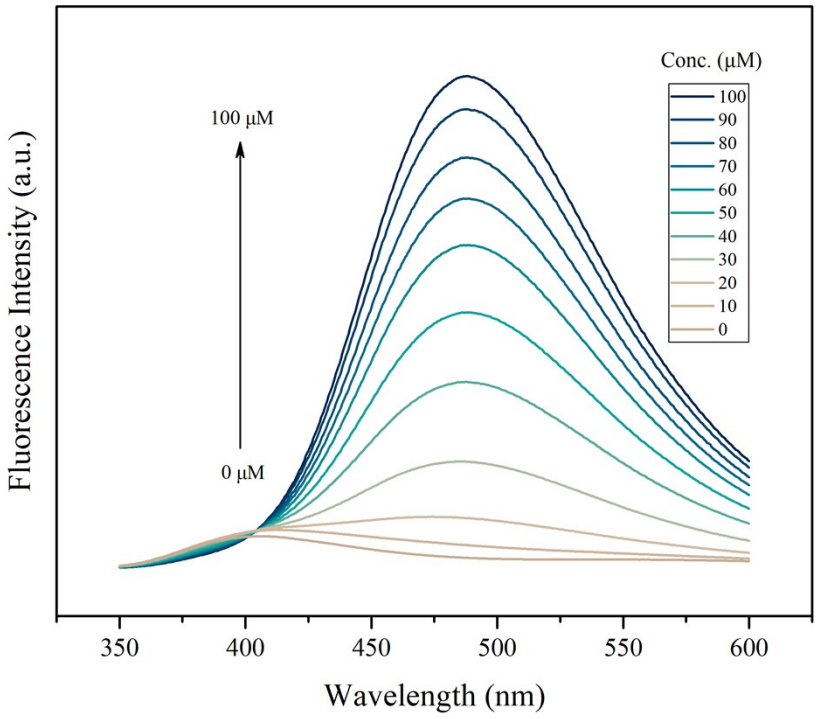

Figure S30 Fluorescence spectrum of **DiCat**/PBA with increasing concentration of spermidine under optimal detection condition. (concentration of **DiCat** and PBA is fixed to be 100 μM and 200 μM respectively)

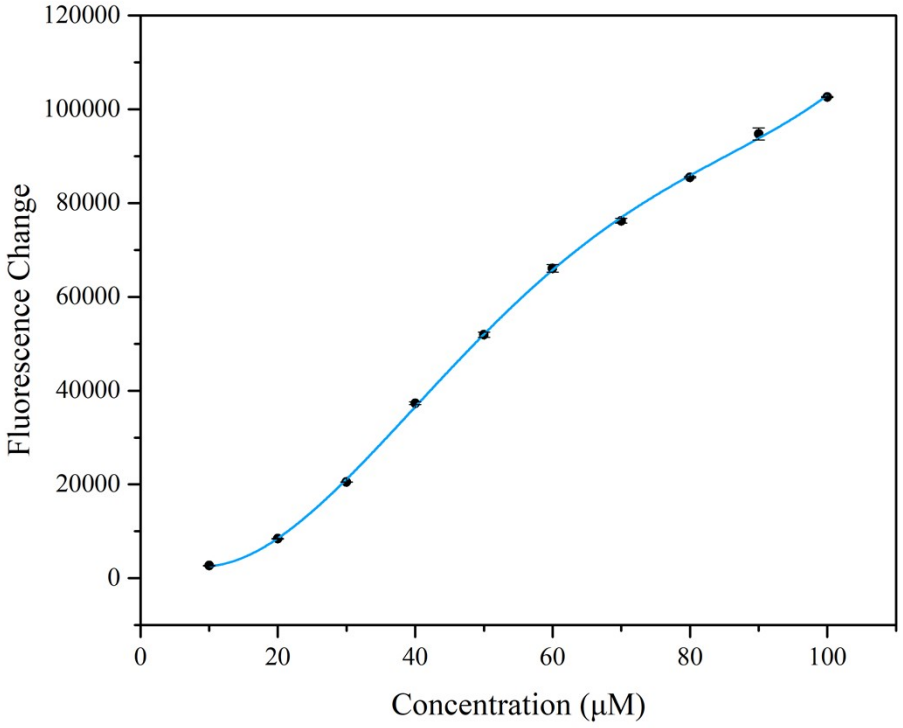

Figure S31 Polynomial regression of fluorescence change versus spermidine concentration.

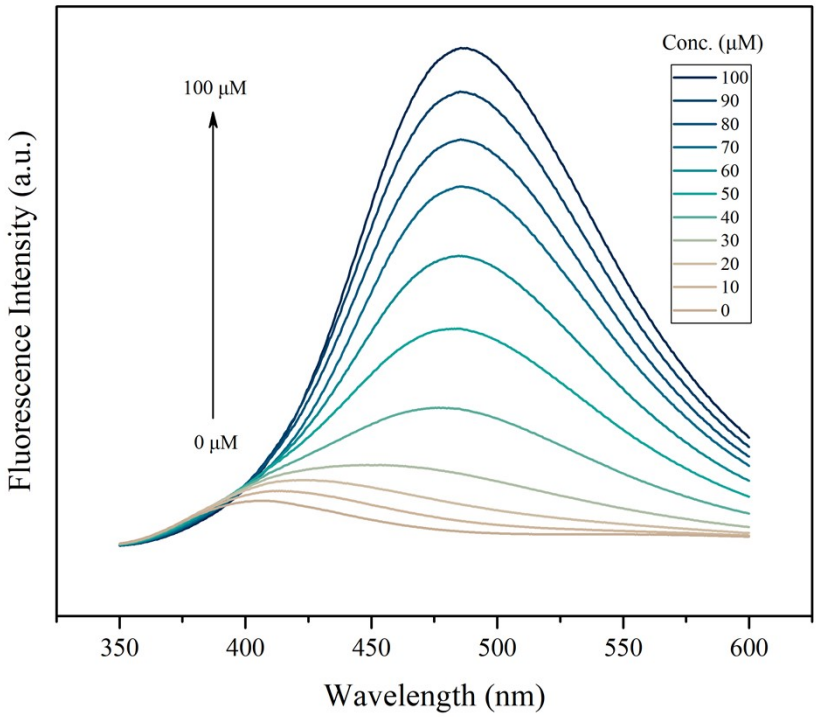

Figure S32 Fluorescence spectrum of **DiCat**/PBA with increasing concentration of tyramine under optimal detection condition. (concentration of **DiCat** and PBA is fixed to be 100 μM and 200 μM respectively)

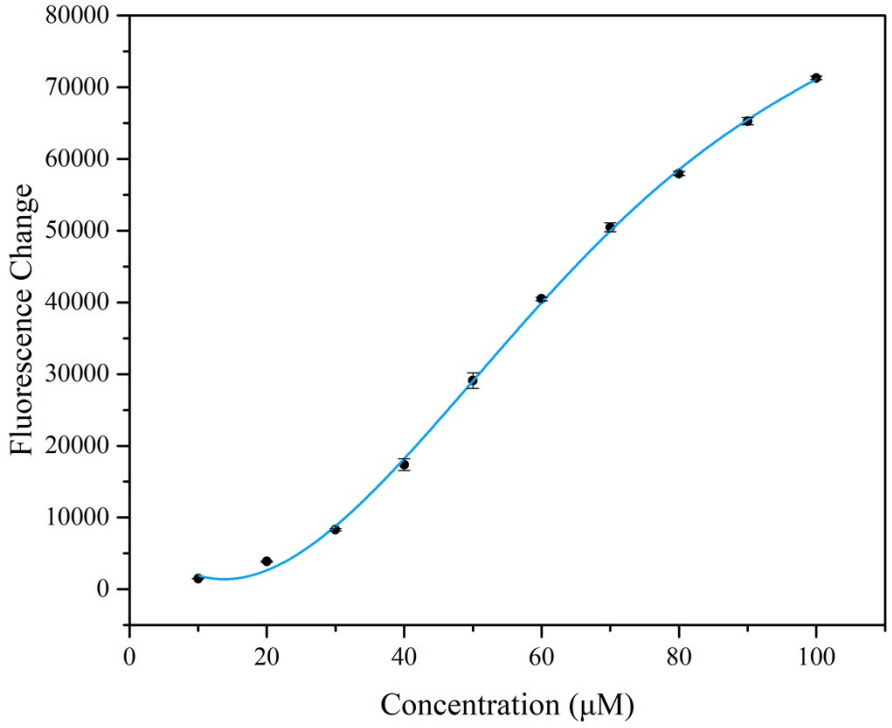

Figure S33 Polynomial regression of fluorescence change versus tyramine concentration.

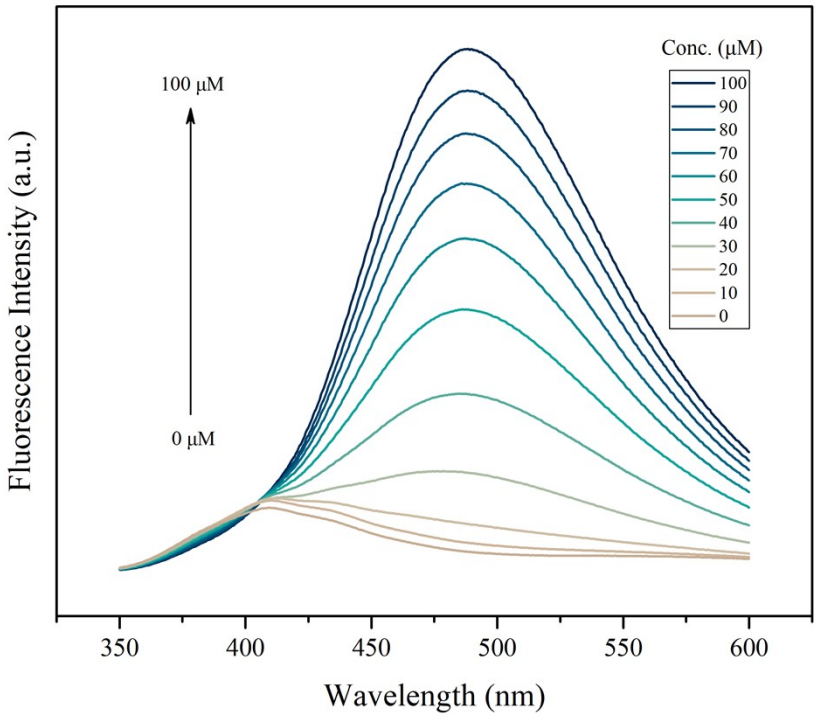

Figure S34 Fluorescence spectrum of **DiCat**/PBA with increasing concentration of phenylethylamine under optimal detection condition. (concentration of **DiCat** and PBA is fixed to be 100 μM and 200 μM respectively)

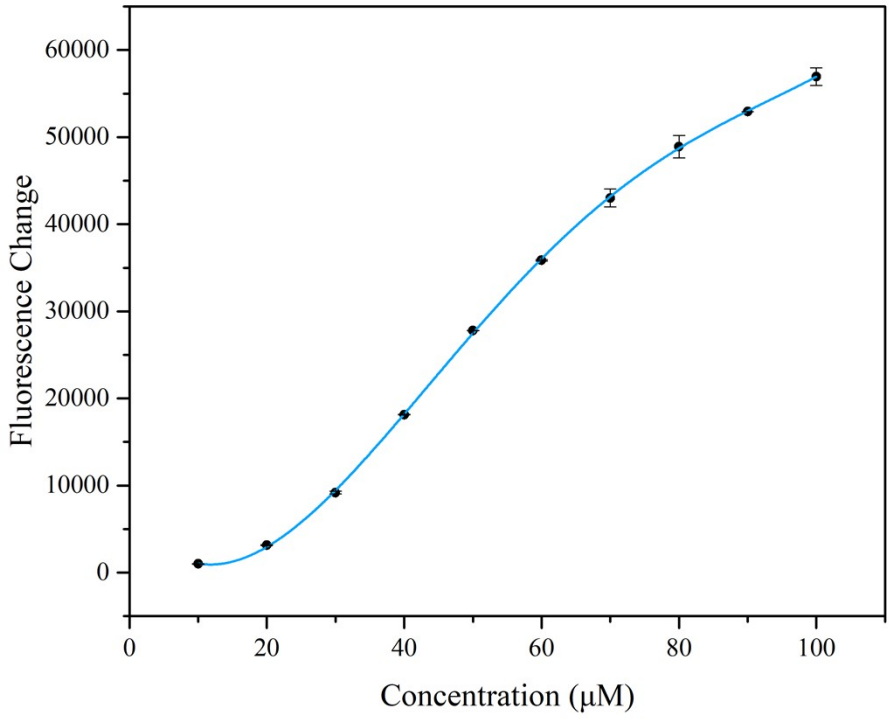

Figure S35 Polynomial regression of fluorescence change versus phenylethylamine concentration.

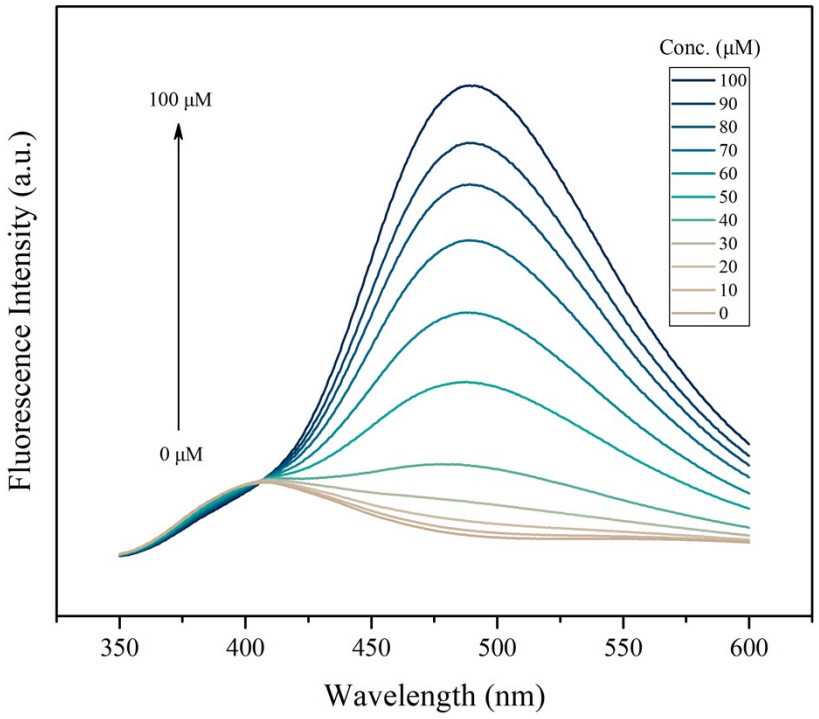

Figure S36 Fluorescence spectrum of **DiCat**/PBA with increasing concentration of histamine under optimal detection condition. (concentration of **DiCat** and PBA is fixed to be 100 μM and 200 μM respectively)

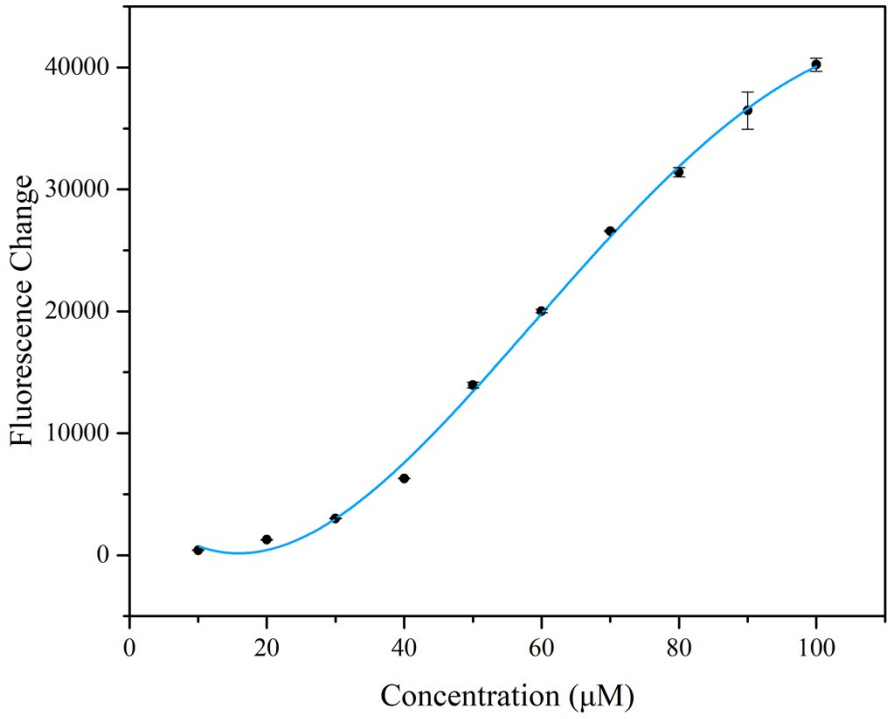

Figure S37 Polynomial regression of fluorescence change versus histamine concentration.

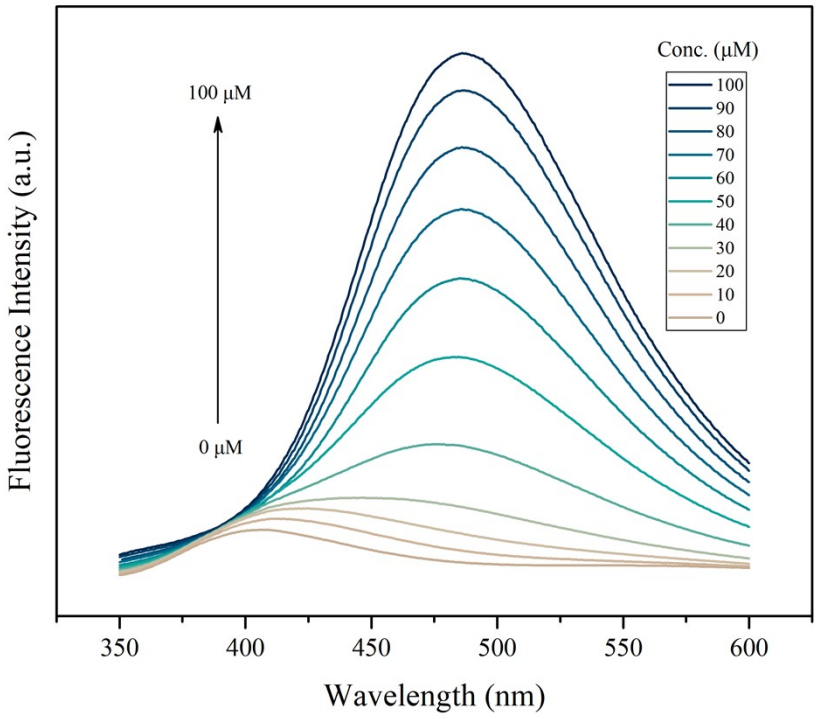

Figure S38 Fluorescence spectrum of **DiCat**/PBA with increasing concentration of tryptamine under optimal detection condition. (concentration of **DiCat** and PBA is fixed to be 100 μM and 200 μM respectively)

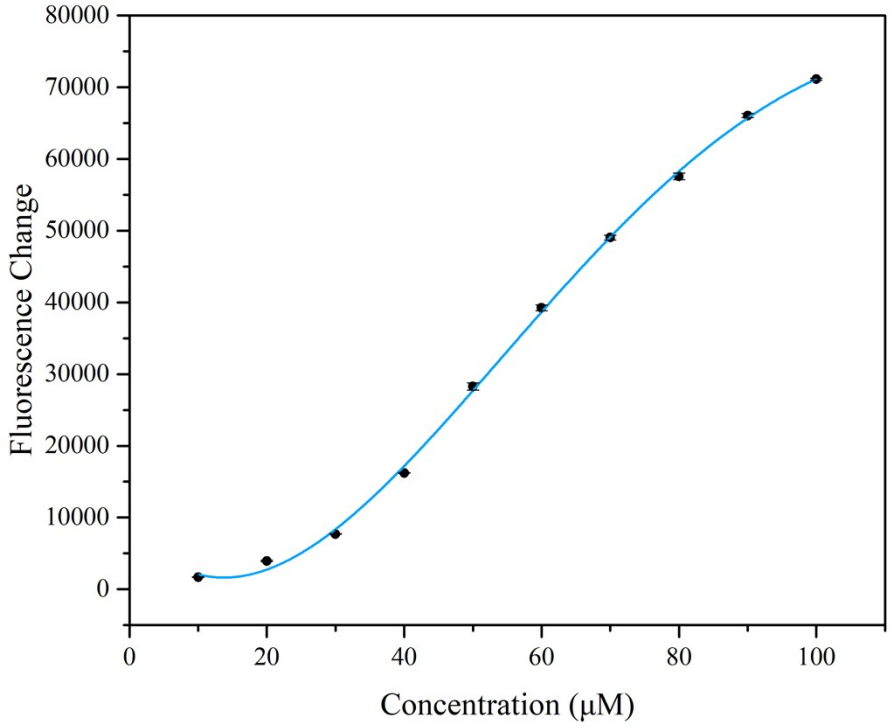

Figure S39 Polynomial regression of fluorescence change versus tryptamine concentration.

Selectivity of this detection protocol

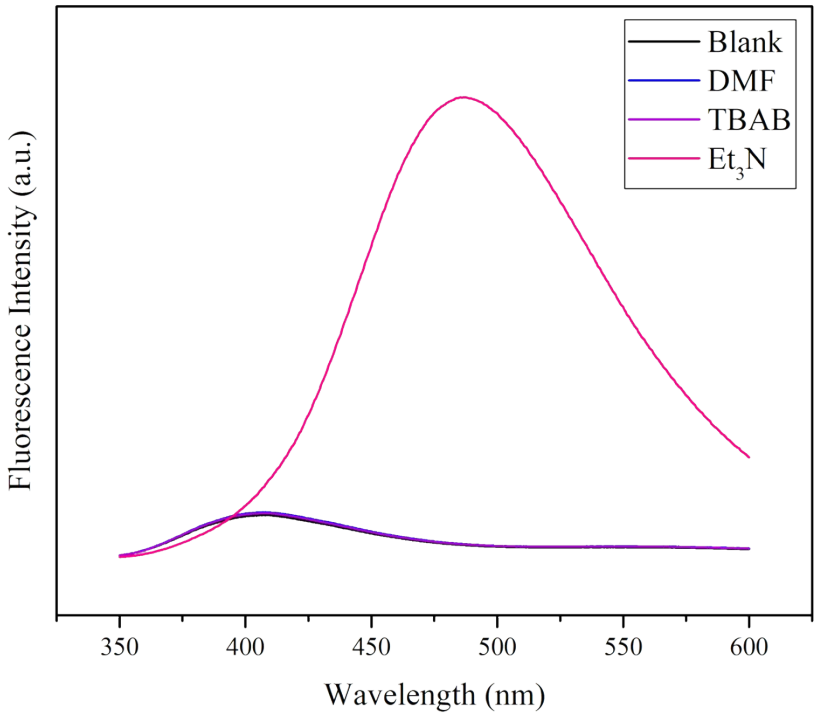

Figure S40 Fluorescence spectrum of **DiCat**/PBA with DMF (100 μM) , TBAB (100 μM) , and Et_3N (100 μM) under optimal detection condition. (concentration of **DiCat** and PBA is fixed to be 100 μM and 200 μM respectively)

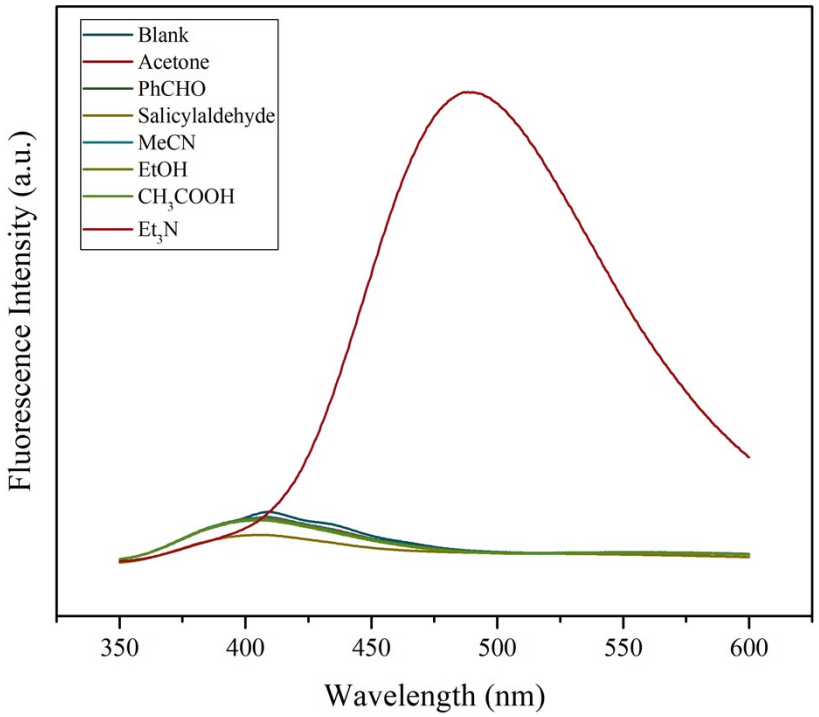

Figure S41 Fluorescence spectrum of **DiCat**/PBA with addition of other common water-soluble organic compounds compared with Et_3N. (with the substance concentration of 100 μM; optimal detection condition is used as concentration of **DiCat** and PBA is fixed to be 100 μM and 200 μM respectively)

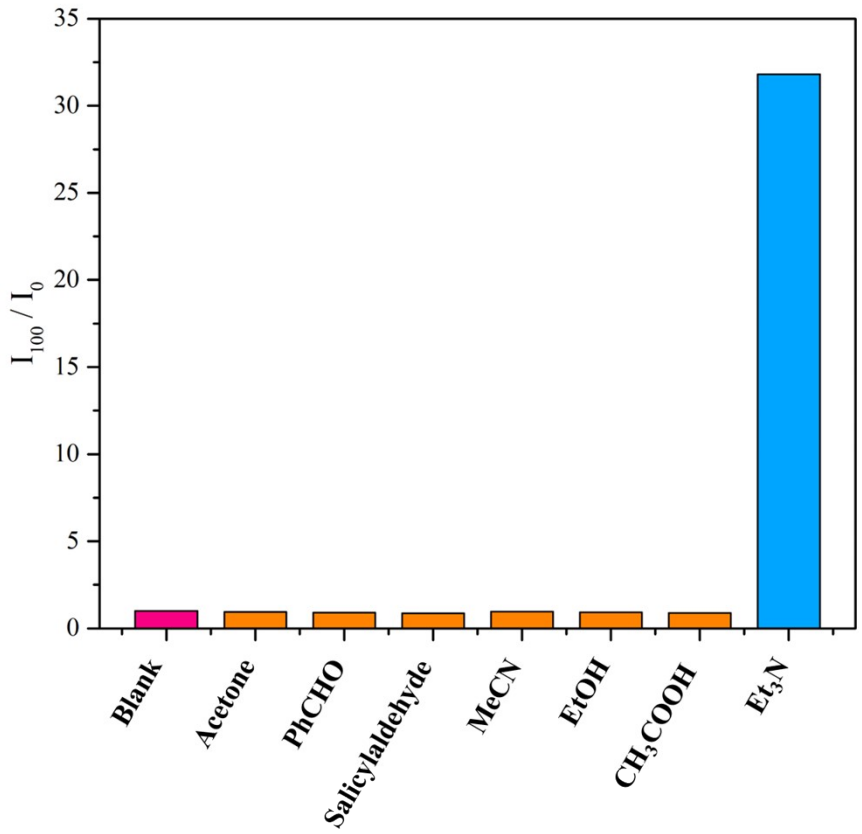

Figure S42 Relative response intensity of **DiCat**/PBA towards different water-soluble organic compounds. (detection condition is the same as shown in **Figure S41**, fluorescence intensity at 488 nm is taken for comparison)

Computational details

Density functional theory (DFT) calculations were carried out with B3LYP functional and 6-31G* basis set for structural optimization of **DiCat**. Detailed atomic coordinates were listed below.

Table S1 Atomic coordinates within the optimal molecular structure of **DiCat**.

Atom Type	x	y	z
C	-1.35601	-1.73323	-1.00533
C	-0.00869	-2.08637	-1.22635
C	1.00394	-1.22858	-0.86479
C	0.71847	0.01318	-0.23317
C	-0.65749	0.3849	-0.02707
C	-1.69875	-0.51647	-0.44079
C	1.76005	0.9133	0.182
C	1.41766	2.13155	0.74292
C	0.07008	2.48716	0.95844
C	-0.94308	1.62892	0.59962
C	-3.14174	-0.1811	-0.29319
C	3.20324	0.57649	0.04128
C	4.07392	1.43814	-0.63851
C	5.43867	1.1588	-0.73262
C	5.96209	0.01168	-0.14392
C	5.09783	-0.85753	0.54573
C	3.74082	-0.57888	0.63805
C	-3.69949	0.96654	-0.87513
C	-5.06489	1.23511	-0.77207
C	-5.90348	0.3613	-0.08516
C	-5.3555	-0.79426	0.49792
C	-3.99604	-1.06112	0.39369
O	-7.23658	0.6307	0.01588

O	-6.25906	-1.59772	1.1607
O	7.29547	-0.25908	-0.23789
O	5.7065	-1.96101	1.10573
H	-2.14707	-2.40602	-1.32539
H	0.22505	-3.03082	-1.71073
H	2.0348	-1.49011	-1.07416
H	2.20918	2.80512	1.05947
H	-0.16397	3.43575	1.43424
H	-1.97421	1.89526	0.80057
H	3.67406	2.33056	-1.1103
H	6.11454	1.82008	-1.26556
H	3.08915	-1.25381	1.189
H	-3.05984	1.64729	-1.42796
H	-5.50139	2.11859	-1.22706
H	-3.58419	-1.95438	0.85933
H	-7.64433	-0.08886	0.52703
H	-5.79917	-2.36119	1.53988
H	7.46092	-1.09099	0.23736
H	5.04608	-2.49671	1.56954

We calculated the excited electronic structure of the proposed tetra-coordinated boronic intermediate while **DiCat**/PBA ensemble interacting with Et_3N. TDDFT method under PBE0-D3/def2-TZVP level was taken to obtain the excited energy, oscillator strength and emission spectrum of the given structure. All the calculations were performed using Gaussian 16 program. The natural transition orbitals (NTOs) and the contributions of molecular orbital transitions were obtained by electron excitation analysis from the transition density matrix of TD-DFT calculation using Multiwfn program[s1]. The SMD (Solvation Model Based on Density) [s2] implicit solvent model was used to describe the solvation effect of tetrahydrofuran and water. The visualization of the frontier molecular orbitals and natural transition orbitals were also rendered using Visual Molecular Dynamic program (VMD)[s3].

Ref.

[s1] T. Lu, F. Chen, *J. Comput.l Chem* **2012**, *33*, 580.

[s2] A. V. Marenich, C. J. Cramer and D. G. Truhlar, *J. Phys. Chem. B*, **2009**, *113*, 6378–6396.
[s3] W. Humphrey, A. Dalke, K. Schulten, *J. Mol. Graphics* **1996**, *14*, 33.